Hydration Kinetics of Calcium Aluminate Cement with Calcium Sulfate Hemihydrate in Presence of Li^+ and Tartaric Acid

F. Goetz-Neunhoeffer
Department of Mineralogy, University of Erlangen-Nuremberg, Germany

Abstract:

Explained in the present paper are the reaction mechanisms responsible for the acceleration or retardation of the hydration of CA - the principal phase in calcium aluminate cement - in mix with $C\bar{S}H_{0.5}$ (calcium sulfate hemihydrate) in presence of Li^+ or tartaric acid. Ettringite is the major phase forming during hydration. Normalized quantitative phase analysis of aqueous pastes by XRD methods in combination with heat flow calorimetry has provided new evidence about the hydration processes. The time-dependent heat flow can be correlated clearly with the dissolving process of the CA and $C\bar{S}H_{0.5}$. When Li^+ is added $Li_2Al_4(OH)_6[(OH)_2 \cdot nH_2O]$ is formed as a reactive intermediate compound that is consumed and then formed again. Li^+ acts here as a catalyst for ettringite formation. On addition of tartaric acid a sparingly soluble calcium tartrate is formed which tends to retard hydration. This effect of tartaric acid ceases as soon as equilibrium is established between calcium tartrate in the solid phase and in the solution.

1 Introduction

Hydraulic active calcium aluminate cements (CACs) were first introduced for building purposes at the beginning of the 20th century. The first patent for a fused limestone-bauxite cement appeared in 1888 [1] but the real starting signal for industrial application was given by the patent registered by Bied [2] in 1909. The hydraulic properties of CACs are attributed to monocalciumaluminate (CA), the main phase of all kinds of calcium aluminate cements.

CACs with different Fe-contents are used in a wide range of formulations for building chemistry applications because of their very rapid early strength. Most formulations with CAC in the mixture are combined with inorganic and organic additives and non reactive aggregates. Where such additives are not present, the reaction mechanisms are mainly dependent on a combination of factors such as homogenisation, grain size, hydration temperature, and w/s values [3]. But there is a growing interest among those concerned with the industrial applications of CACs in acquiring a knowledge of the actual scientific principles underlying the influence of the usual additives, such as lithium carbonate and carbonic acids, on workability and setting time in technical products like smoothing cements, tile adhesives or joint compounds. Hitherto, the very complex dry mortar

formulations have been, to a large extent, arrived at by processes of trial and error.

Earlier investigations concerning hydration of pure monocalciumaluminate (CA) from solid state synthesis and of CA as major phase in calcium aluminate cements (CAZ) were able to demonstrate that, when Ca^{2+}-rich additives were present, the reproducibility of hydration of CA was in every case significantly improved [4-6]. Moreover, the points in time of maximum heat flow were attained earlier with Ca^{2+}-rich additives than with pure CA [7].

The presence of Li_2CO_3 in the mixing water for hydration of CA or CAC results in the formation of an intermediate phase ($Li_2Al_4(OH)_6[(OH)_2 \cdot nH_2O]$, LiAl-DLH). The formation of the intermediate LiAl-DLH acts as a catalyst and strongly improves the further dissolution of CA. The outcome of this is an increase of the reaction rate in the pastes, correlated with formation of C_2AH_8 in neat CA and CAC pastes. The model for sulfate-free reaction [8, 9] is based on quantitative data from X-ray powder diffraction (XRPD) and heat flow calorimetry. Both methods yield very good reproducible data after calibration, measurement and standardisation [10, 11]. By combination of both analytical methods, the influence of additives can be clearly shown and interpreted.

For the investigations with mixtures of $C\bar{S}H_{0.5}$ (calcium sulfate hemihydrate) presented below, two different cements were employed: Fe-free CAC and synthetic Fe-rich calcium aluminate cement (SCAFC). A mass ratio of CaO/SO_3 = 2.1 was chosen for all cements. Hydration in mixes with calcium sulfate hemihydrate ($C\bar{S}H_{0.5}$), in each case with and without Li^+ and tartaric acid, was monitored by heat flow calorimetry and in-situ XRD. Rietveld refinement of the in-situ recorded XRD pattern of the hydrating pastes was used in order to acquire quantitative data regarding the dissolution of CA and $C\bar{S}H_{0.5}$ during the first 24 h of hydration. In consideration of the non-crystalline part in the pastes – H_2O and amorphous aluminium hydroxyl hydrate – the quantitative data of the crystalline from Rietveld refinement and the amorphous phases were standardised to 100 ma.%.

2 Experimental

2.1 Syntheses of the Fe-rich SCAFC

The SCAFC was produced in such a manner that its chemical composition was similar to that of „standard-grade“ CAFC as defined in [12, p. 713], but in the reduced system $CaO\text{-}Al_2O_3\text{-}Fe_2O_3\text{-}SiO_2$. This yielded a phase assemblage of CA - ferrite phase - C_2S - gehlenite. The raw materials for SCAFC (Table 1), reagent grade chemicals $CaCO_3$, Al_2O_3, Fe_2O_3 and SiO_2, were mixed in a disk mill and calcined for 15-17 h in a laboratory furnace at 1250 °C.

Table 1: Chemical composition of the SCAFC (all data in ma%)

CaO	Al_2O_3	Fe_2O_3	SiO_2	C/A-ratio
39.5	39.5	15	6	1

Raw meal was filled into alumina crucibles after grinding and placed in a laboratory furnace. SCAFC were synthesized according to a defined temperature program starting from 700 °C with a heating rate from 1 °C/min up to 1450 °C. After dwell time (2 h) at 1450 °C, the melt was subsequently cooled with 25 °C/min down to 1200 °C and then quenched in air. The cooling rate was determined by in-situ measurement of temperature via Pt-Rh thermocouple. Spectroscopic analysis of ferrous iron content was < 1 ma% throughout for the SCAFC samples.

2.2 Quantitative mineralogical phase analysis of the cements

XRD data of the Fe-free CAC and the synthetic SCAFC were collected using a D5000 Bragg-Brentano diffractometer with $Cu_{K\alpha}$-radiation. Preparation of the investigated powders, which were ground in a disc mill to get the required grain sizes (≤ 36 µm) for X-ray powder diffraction, was performed by means of frontloading technique. In order to guarantee representative specimen, the cements were homogenised and divided by a laboratory sampler.
For XRD data collection for Rietveld analysis, the fixed slit arrangement and secondary graphite monochromator were utilised. The instrumental parameters for the D5000 diffractometer are shown in Table 2.
Lattice and structural parameter refinement by Rietveld analysis with fundamental parameter approach (TOPAS Version 2.1, BRUKER AXS) was employed for crystallographic characterisation.

2.3 In-situ XRD analysis of the hydration

The phase evolution in the cement/calcium sulfate pastes with a w/c ratio of 0.5 was investigated by means of in-situ X-ray diffraction at a temperature of 23° C. The pastes were prepared by mixing of the samples with H_2O for 30 s with a stirring machine. After preparation into a special sampleholder, the pastes were covered by a 7µm Kapton-Brand X-ray film. This cover is used to create a closed saturated water vapour atmosphere in the paste. The first measurement was started 3.5 mins after addition of H_2O. The procedure was repeated for 5 preparations. The measurement conditions for the Bruker AXS D8 equipment with a Braun PSD are shown in Table 2.
Quantitative phase analyses and structural refinements were carried out at up to 20 points of time during the first 24 h of hydration, using Topas 2.1 with a suitable fundamental parameter approach. Structural data were derived from ICSD structural database (FIZ, Karlsruhe) [13] and were

refined on the basis of pure phases. For the refinement of the resulting crystalline hydrate ettringite, there was employed a new structural data set which included the hydrogen positions in the structure model [14].

Table 2: Measurement conditions quantitative and in-situ XRD analysis

	Quantitative XRD-analysis (D5000)	In-situ XRD-analysis (D8)
Radiation	Cu Kα	Cu Kα
Tube voltage	40 kV	40 kV
Tube current	30 mA	30 mA
Angular range	10 - 65 °2θ	7 – 34 °2θ
Step width	0,02° 2θ	0,02° 2θ
Time per step	4 s	0,5 s
Divergence slits	0,5°/0,5° Fixed slits	0,5° Primary fixed slit
Time/range	3 h	12 min
Monochromator	Secondary graphite monochromator	Secondary Ni-Filter
Detector	Scintillation counter	Braun OED with anti scatter slit

2.4 Specific surface area

The specific surface area of the technical cement (CAC), of the synthetic Fe-rich cement (SCAFC) and of the $C\bar{S}H_{0.5}$ was determined by the Blaine method (Table 3). Calibration was performed with quartz powder standards of 3980 und 4620 cm^2/g.

Table 3: Specific surface areas (as determined by Blaine method)

Cement	D_x [g/cm^3]	Average value [cm^2/g]	Standard deviation [cm^2/g]	System. error ± 5 % [cm^2/g]
Fe-free CAC	2.99	4360	±40	±220
Fe-rich SCAFC	3.20	3980	±40	±200

2.5 Heat flow calorimetry

For the investigation of the hydration, there was employed a heat flow calorimeter operating in isothermal mode [10,11, 15]. It was possible to investigate simultaneously three samples in flat polystyrene vessels. Data acquisition was conducted by means of the software *OMI* (Dr. Ecker GmbH/Mesicon). The temperature during hydration was kept constant at a value of 23.0± 0.3 °C. Preparation of the pastes was as described in chapter 2.3 for in-situ XRD analysis of the hydration. Table 5 summarises the instrumental parameters.

Table 4: Instrumental parameters of the heat flow calorimeter

Hydration time [h]	24/48/100
Integration time / cell [s]	5
Interval time [s]	19

3 Mineralogical characterisation of the materials used

3.1 Quantitative phase analysis of the cements

3.1.1 Fe-free calcium aluminate cement (CAC)

For the calibration of quantitative phase analysis, all CAC clinker phases which were identified were synthesized from reagent grade chemicals in a laboratory furnace in air. A clinkerspecific Rietveld quantification method was developed by the mixing of synthetic phases with compositions determined by reference to the technical clinker. With this calibration, the values of quantitative phase analysis can be taken for actual values. Table 5 shows the values as determined for Fe-free CAC.

Table 5: Quantitative phase analysis of the Fe-free calcium aluminate cement (CAC)

Phase	Average [ma. %]	s [ma. %]	Min value [ma. %]	Max value [ma. %]
CA	60.3	0.3	59.9	60.8
CA_2	33.5	0.3	33.0	34.0
A	6.2	0.3	5.8	6.7

3.1.2 Synthetic Fe-rich calcium aluminate cement (SCAFC)

It is not possible to determine the Fe-content in ferrite and gehlenite by comparison with synthesized solid solutions from solid state reactions, the cations Si^{4+}-Al^{3+}-Fe^{3+} tending to take each other's places at several atomic sites in the crystal lattices – a factor which may be responsible for the refined distorted lattices. The creation of the Rietveld quantification method was supported, therefore, in the cases of Fe-rich calcium aluminate cement with 6 ma.% SiO_2, by chemical analysis of single grains with electron probe microanalysis [16].

Table 6: Results of the quantitative phase analysis of the SCAFC (* standard deviation of 10 independent preparations)

Phase	Composition of solid solutions	QXRD [ma.%]
Monocalciumaluminate	$CA_{0.94}F_{0.06}$	46.8 ± 1.2*
Ferrite	$C_6A_{1.22}F_{1.78}$	24.8 ± 0.5*
Gehlenite	$C_2A_{0.88}F_{0.12}S$	28.4 ± 0.8*

3.2 Characterisation of the calcium sulfate hemihydrate

The $CaSO_4 \cdot 0.5\ H_2O$ ($C\bar{S}H_{0.5}$) used for the investigation of the mixes of calcium aluminate and calcium sulfate (CaO/SO_3 = 2.1) is one which is commonly so used and which is, moreover, specifically recommended for building chemistry applications (RADDiCHEM 27, Rethmann, Germany). Density is guaranteed with 2.757 g/cm^3. Quantitative XRD analysis proved 99.9 ma.% purity.

3.3 Characterisation of the tartaric acid

According to the manufacturer's documents (UD-Chemie, Germany) the natural tartaric acid used here – namely, L(+) form $C_4H_6O_6$ - is 97-100 % pure. The XRD pattern of the tartaric acid definitely matches the pattern of the ICDD-PDF data set 20-1901. No impurities of other crystalline phases could be detected.

4 Results of the calorimetric investigation

The average heat flow curves of the pastes mixed from the Fe-free CAC and calcium sulfate hemihydrate ($C\bar{S}H_{0.5}$) are shown in Figure 1. The heat flow of the CAC- $C\bar{S}H_{0.5}$-mix (mass ratio CaO/SO_3 = 2.1) with pure deionised H_2O attains values lying between 5 and 10 mW/g with a maximum t_{max} at 5.8 h. The reaction rate in presence of low concentration of Li_2CO_3 (0.2 ma.%) in the mixing water is strongly increased and the maximum heat flow of 48 mW/g is attained after 0.2 h of hydration. The heat flow of the CAC-$C\bar{S}H_{0.5}$-mix with 0.2 ma. % Li_2CO_3 - the same concentration - but additionally 0.2 ma. % tartaric acid is leading to a very different course of hydration. Where the concentration of Li_2CO_3 in the CAC-$C\bar{S}H_{0.5}$-mix is maintained at the same concentration – namely 0.2 ma. % Li_2CO_3 – but there is further added 0.2 ma. % tartaric acid, there results a very different course of hydration: after the initial heat flow, there was determined, due to primary dissolution of CA and $C\bar{S}H_{0.5,}$ a very low heat flow of 0.05 mW/g up to the 6-hour point. Then, the heat flow increased very rapidly up to a level of 23 mW/g at the point of time t_{max1} of 7.21 h. This retarding effect of tartaric acid on t_{max} is very significant and can be observed in different degrees depending upon the tartaric acid's different levels of concentration. Lower concentrations of tartaric acid have a less retarding effect than higher concentrations but there could be determined no linear correlation between concentration and retarding effect [9]. Another difference between the heat flow curves with and without tartaric acid is the occurrence of a second maximum at t_{max2} of 10.75 h. All determined times of maximum heat flow for the CAC-$C\bar{S}H_{0.5}$-mix with 0.2 ma. % Li_2CO_3 and 0.2 ma.% tartaric acid are very good reproducible, with a standard deviation of only 0.08h.

With addition of Li_2CO_3 and tartaric acid, the values for the overall heat of hydration after 24 h decrease (see Figure 1 and Table 7) from 317 J/g (without additive) to 262 J/g (0.2 ma.% Li_2CO_3) and finally to 217 J/g (0.2

ma.% Li_2CO_3 and 0.2 ma.% tartaric acid). This finding tends to contradict the observation that very low heat flows of between 0.4 and 0.8 mW/g at 24h mean that hydration is nearly completed. But in the case that additives are used, dissolution of CA and $C\bar{S}H_{0.5}$ was less advanced than without additives.

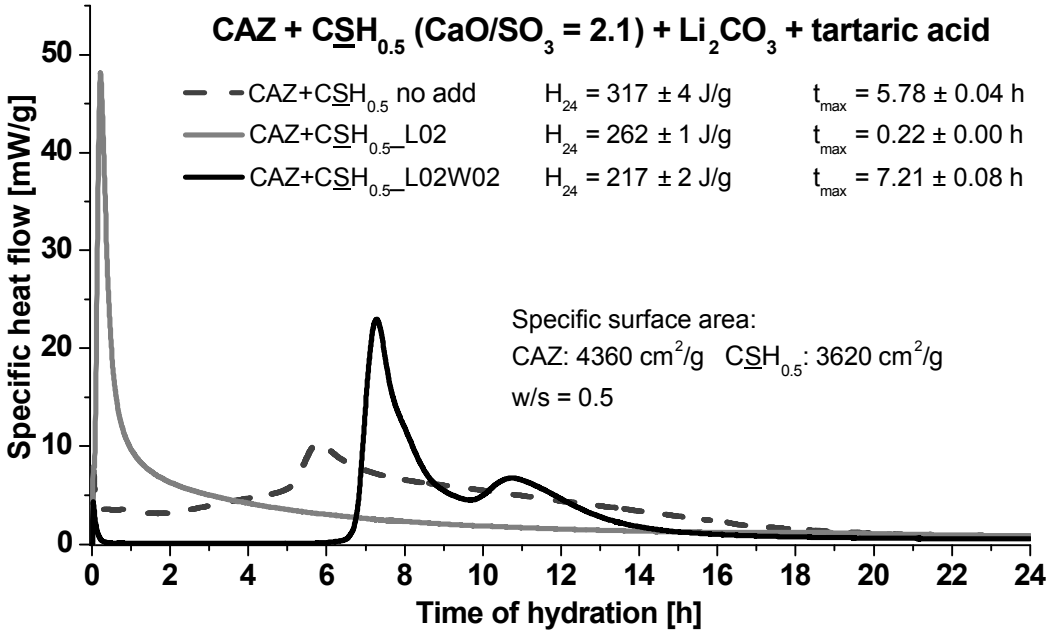

Figure 1: Heat flow of CAC-$C\bar{S}H_{0.5}$ mixes without and with Li_2CO_3 and tartaric acid in deionised H_2O (w/s = 0.5; T=23 °C)

In Figure 2, there are shown the average heat flow curves of the pastes mixed from the Fe-rich synthetic SCAFC and $C\bar{S}H_{0.5}$ (CaO/SO_3 = 2.1). The maximum heat flow of synthetic Fe-rich calcium aluminate cement in mix with the calcium sulphate is, in spite of comparable specific surface areas, less strongly retarded than is the case with Fe-free calcium aluminate cement. This difference was detected for a technical Fe-rich calcium aluminate cement but at a lower scale [9]. By contrast, the influence of Li_2CO_3 is again very distinct. The maximum of heat flow is shifted to 0.42 h for the hydration of the SCAFC-$C\bar{S}H_{0.5}$ mix with 0.2 ma. % Li_2CO_3 dissolved in the mixing water. But there is no second maximum point of heat flow to be observed here.

The rise of the heat flow to its maximum, and its descent from this point, are very comparable for the reactions of the SCAFC-$C\bar{S}H_{0.5}$ mix with 0.2 ma. % Li_2CO_3 and with $C\bar{S}H_{0.5}$ mix with 0.2 ma. % Li_2CO_3 together with 0.2 ma. % tartaric acid. The faster increase to maximum heat flow is probably due to the addition of Li_2CO_3.

The addition of Li_2CO_3 and tartaric acid again led to a decrease of the values for the overall heat of hydration after 24 h (see Figure 2) from 293 J/g (without additive) to 217 J/g (0.2 ma.% Li_2CO_3) and to 224 J/g (0.2 ma.% Li_2CO_3 and 0.2 ma.% tartaric acid).

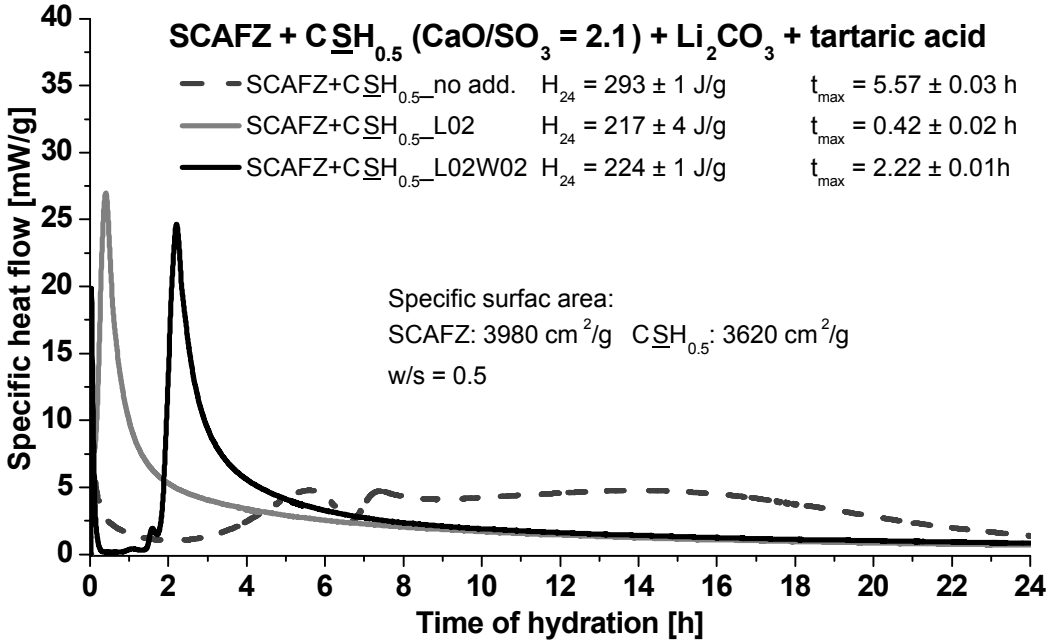

Figure 2: Heat flow of SCAFC-C$\bar{S}$H$_{0.5}$ mixes without and with Li_2CO_3 and tartaric acid in deionised H_2O (w/s = 0.5; T=23 °C)

5 Results and discussion of the quantitative phase analysis (Rietveld results after standardisation with H_2O to 100 ma. %)

Hydration of the Fe-free CAC and of the Fe-rich synthetic SCAFC without additives and in presence of 0.2 ma.% Li_2CO_3 and 0.2 ma.% tartaric acid display a very good comparability with one another. Ferrite influence at this stage of hydration could not be determined by XRD analysis. Reactions of both cements are dominated by the dissolution of the main phase CA and $CA_{0.94}F_{0.06}$ respectively with C$\bar{S}$H$_{0.5}$ and the formation of ettringite and very minor gypsum. Only plotted in Figure 3 is the kinetics of ettringite and gypsum formation in the different cements alone. For the highest values of ettringite, the dissolution of CA and C$\bar{S}$H$_{0.5}$ does not continue, but both phases are still detected in the paste.

Two reactions occur continuously during the hydration of the mixes, *Equation 1* only in presence of Li_2CO_3:

3CA + 3 C$\bar{S}$H$_{0.5}$ + 2 Li^+ +*n* H_2O =>

==.LiAl-DLH==>

=> C_3A*3C$\bar{S}$H$_{32}$ + 2AH_3 + 2 Li^+ + *m* H_2O*Equation 1*

C$\bar{S}$H$_{0.5}$ + 1.5 H_2O => C$\bar{S}$H$_2$ *Equation 2*

Dissolution of CA and $CA_{0.94}F_{0.06}$ respectively for the Fe-rich SCAFC is catalysed by Li^+ by the formation of the intermediate hydrate LiAl-DLH ($=Li_2Al_4(OH)_{12}[(OH)_2 \cdot 3H_2O]$). This intermediate hydrate acts to prevent the formation of an insoluble Al-hydroxyl-hydrate layer around the CA particles, said layer tending indeed to form in the absence of Li^+ [8, 9]. The reaction rate of Equ.1 which tends to lead to ettringite formation , is strongly correlated with the concentration of Li_2CO_3.

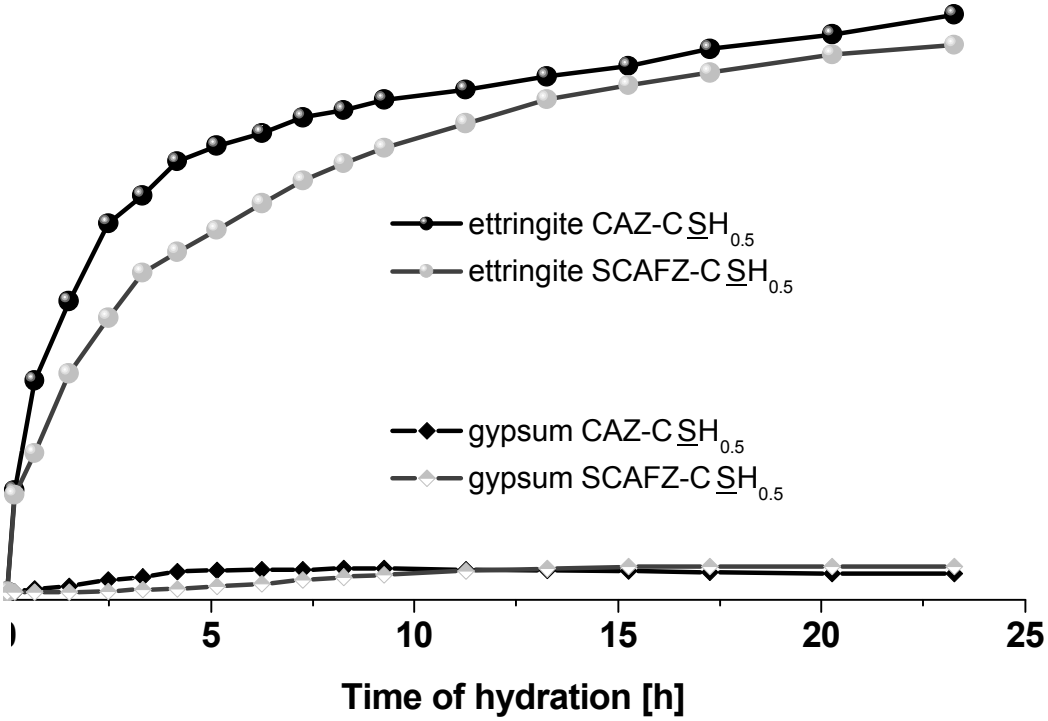

Figure 3: Standardised quantities of ettringite and gypsum formation during 24 h of hydration in mix CAC-C$\bar{S}H_{0.5}$ and in mix SCAFZ-C$\bar{S}H_{0.5}$ with 0.2 ma. % Li_2CO_3 at w/s=0.5

Figure 4 shows the influence of the additives and their combination on the hydration kinetics of the mix CAC-C$\bar{S}H_{0.5}$. The same principal results were determined for the synthetic Fe-rich SCAFC but are not presented here. Where no additive is present the mix CAC-C$\bar{S}H_{0.5}$, the formation of ettringite is nearly linear up to14 h and then the slope of the curve tends to decline. Ettringite is still forming after 24 h, but only in very low amounts compared with the overall quantity of 41 ma.%. At the same time, 17 ma.% of the CA is dissolved (Table 7). Ettringite formation with 0.2 ma.% Li_2CO_3 is characterised by a very high slope of the increasing standardised quantities from 0 to 5 h, after which the curve declines. Finally, after 24 h, an average quantity of 38 ma.% ettringite is formed and 15 ma.% of CA is dissolved. The hydration of the mix CAC-C$\bar{S}H_{0.5}$ with 0.2 ma.% Li_2CO_3 and 0.2 ma.% tartaric acid resulted in a very different curve for ettringite formation. Up to 3.5 h after mixing, no ettringite could be observed in the paste but then ettringite began to form very rapidly –

displaying nearly the same slope as the hydration of the mix without tartaric acid. It follows that this increase must be due to the addition of Li_2CO_3. After 24 h, the lowest average quantity of ettringite (30 ma.%) was determined (Figure 4) by Rietveld quantification of five independent measurements. Therefore, the lowest CA dissolution is combined with the addition of 0.2 ma.% Li_2CO_3 and 0.2 ma.% tartaric acid to the CAC-$C\bar{S}H_{0.5}$-mix.

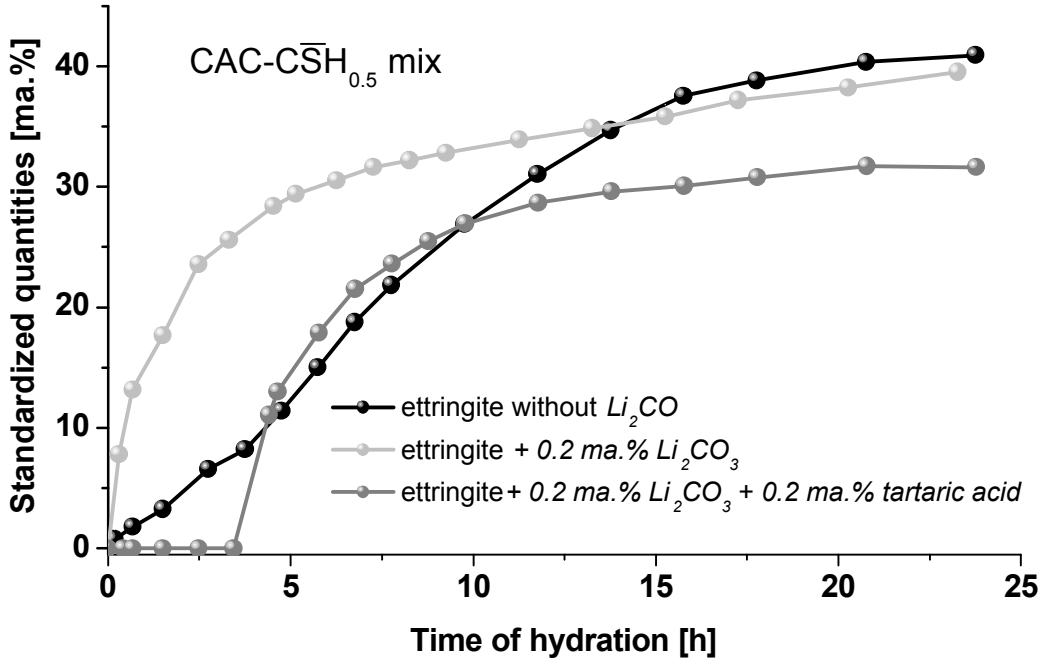

Figure 4: Standardised quantities of ettringite formation during 24 h of hydration of the CAC-$C\bar{S}H_{0.5}$-mixes with and without additives (0.2 ma. % Li_2CO_3/ 0.2 ma.% tartaric acid) at w/s=0.5

Table 7: Heat of hydration and average ettringite and CA contents, after 24 h, of the mix CAZ-$C\bar{S}H_{0.5}$ in dependence on the additives Li_2CO_3 und tartaric acid for w/s=0.5

Additive	Heat of hydration H_{24} [J/g]	Average ettringite [ma.%]	Average CA dissolution [ma.%]
without	317	41	17
0.02 Li_2CO_3	322	42	16
0.2 Li_2CO_3	262	38	15
0.2 Li_2CO_3+0.05 tartaric acid	243	34	13
0.2 Li_2CO_3+0.2 tartaric acid	217	30	12

(All concentrations in ma. % with respect to the solid.)

6 Conclusion

The results led to a hydration model for systems containing CA and $C\bar{S}H_{0.5}$. The most complex model proved necessary as regards the combination of Li_2CO_3 - which turned out to be a very effective accelerator with respect to CA dissolution - with tartaric acid. Even very low concentrations of Li_2CO_3 tend to significantly alter the reaction rate of CA dissolution. The course of the heat evolution is determined by the dissolution rates of CA and $C\bar{S}H_{0.5}$.

Figure 5 shows the model for hydration of CA and $C\bar{S}H_{0.5}$ where the additive Li_2CO_3 is present. Immediately after mixing, the $C\bar{S}H_{0.5}$ and CA are dissolved, resulting, according to Equations 1 and 2, in the formation of the hydrates ettringite and gypsum. Lowreactive CA and highly reactive $C\bar{S}H_{0.5}$ tend to promote gypsum reaction (Equation 2). Whereas high CA reactivity and low $C\bar{S}H_{0.5}$ reactivity may result in monosulfate instead of ettringite, this latter needing less sulfate for its formation. In the case of the presence of Li^+, there tends to be a layer of Al-hydroxyl-hydrate intergrown with the phase LiAl-DLH covering the CA grains. This phase is of very low crystallinity and forms, together with calcium and sulfate, the typical ettringite prisms around the CA grain; it may even precipitate into the solution surrounding the grain. Within 24 h, much more ettringite is formed by continuous dissolution of further CA and $C\bar{S}H_{0.5}$. The concentration of Li^+ determines the quantity of LiAl-DLH phase in the paste, which in turn determines the rate of ettringite formation.

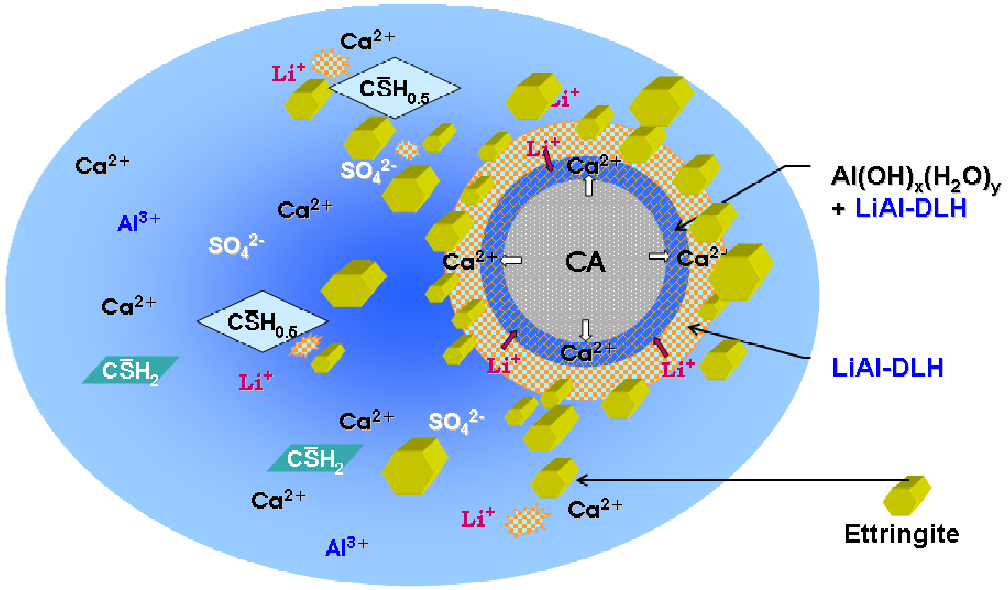

Figure 5: Model for catalytic ettringite formation from CA and $C\bar{S}H_{0.5}$ in presence of Li^+ and LiAl-DLH respectively

7 Literature

[1] G.J. Senelus, T. Gibb, J.C. Swann, H. Smith, W. Whamond, British Patent 10312, 1888.

[2] J. Bied, British Patent 8193, 1909.

[3] F. Goetz-Neunhoeffer & J. Neubauer,: Effect of inorganic admixtures on the early hydration of Monocalciumaluminate ($CA_{1-x}F_x$), *Proceedings of the 11th International Congress on the Chemistry of Cement, Durban 2003 (South Africa)*, G. Grieves & G. Owens (Eds.), Tech Books International, ISBN: 81-88305-10-3, Volume 2, 2004, pp. 1045-1059.

[4] M. Schmid , F. Goetz-Neunhoeffer & J. Neubauer: Effect of $Ca(OH)_2$ on hydration behavior of synthetic Calcium Aluminate Cements, *Proceedings of the 11th International Congress on the Chemistry of Cement, Durban 2003 (South Africa),* G. Grieves & G. Owens (Eds.), Tech Books International, ISBN: 81-88305-10-3, Volume 2, 2004; pp. 973-985.

[5] M. Schmid, F. Götz-Neunhoeffer & J. Neubauer,: Hydratation von eisenfreiem Tonerdezement unter Einfluss von Portlandit und Li_2CO_3-Lösung, *GDCh-Monographie Bauchemie*, Band 25, 2002, pp. 176-178.

[6] R. Enderle, F. Götz-Neunhoeffer & J. Neubauer: Der Einfluss des anorganischen Additivs $C_{12}A_7$ auf das Hydratationsverhalten von Monocalciumaluminat, *GDCh-Monographie Bauchemie*, Bd 25, 2002, pp. 179-181.

[7] F. Götz-Neunhoeffer, Der Einfluss Ca-reicher Verbindungen auf das Hydratationsverhalten von Monocalciumaluminat (CA), *Tagungsbericht der 15. Internationalen Baustofftagung ibausil,* Band 1, 2003, pp. 467-478.

[8] F. Götz-Neunhoeffer, Kinetik der Hydratation von Calciumaluminatzement mit Zusatzstoffen, *ZKG-International*, , Volume 58, No. 4, 2005, 65-72.

[9] F. Götz-Neunhoeffer, Modelle zur Kinetik der Hydratation von Calciumaluminatzement mit Calciumsulfat aus kristallchemischer und mineralogischer Sicht, *Erlanger Forschungen, Reihe B, Naturwissenschaften und Medizin, Band 29*, ISBN: 3-930357-78-X, 2006, 247 p.

[10] J. Neubauer & F. Goetz-Neunhoeffer: Efficiency of highly sensitive heat flow calorimetry in examination of OPC hydration, *Proc. of the 24th Int. Conference on Cement Microscopy, San Diego*, 2002, pp. 58-68

[11] J. Neubauer & F. Götz-Neunhoeffer, In-situ XRD-Analyse und Wärmeflusskalorimetrie am Beispiel der Zementhydratation, *GDCh-Monographie Bauchemie*, 2005, pp. 150-163.

[12] K.L. Scrivener & A. Capmas, Calcium Aluminate Cements, in: P.C. Hewlett (Ed.), Lea's Chemistry of Cement and Concrete, 4th Edition, John Wiley and Sons, New York, 1998, pp. 707-778.
[13] FIZ Karlsruhe, ICSD, Inorganic Crystal Structure Database, 2005/2.
[14] F. Goetz-Neunhoeffer & J. Neubauer, Refined ettringite structure for quantitative X-Ray diffraction analysis, *Journal of Powder Diffraction*, Vol. 21, 1, 2006, 4-11.
[15] H.J. Kuzel, Ein leistungsfähiges Wärmeleitungskalorimeter, TIZ Fachberichte, Vol. 108, No. 1, 1984, 46-51.
[16] M. Schmid, F. Goetz-Neunhoeffer & J. Neubauer, Quantitative phase analysis of synthetic CAC from melts in the system CaO-Al_2O_3-Fe_2O_3-SiO_2. *Proc. of the 27th Int. Conference on Cement Microscopy, Victoria, Canada*, 2005, 15 pp.